GRIDLESS TWO-DIMENSIONAL DOA ESTIMATION WITH L-SHAPED ARRAY BASED ON THE CROSS-COVARIANCE MATRIX

Xiaohuan Wu[1], *Wei-Ping Zhu*[1,2] *and Jun Yan*[1]

[1]Key Lab of Broadband Wireless Communication and Sensor Network Technology,
Nanjing University of Posts and Telecommunications, Nanjing, China
[2]Department of Electrical and Computer Engineering,
Concordia University, Montreal, Canada
Email: {2013010101, zwp, yanj}@njupt.edu.cn

ABSTRACT

The atomic norm minimization (ANM) has been successfully incorporated into the two-dimensional (2-D) direction-of-arrival (DOA) estimation problem for super-resolution. However, its computational workload might be unaffordable when the number of snapshots is large. In this paper, we propose two gridless methods for 2-D DOA estimation with L-shaped array based on the atomic norm to improve the computational efficiency. Firstly, by exploiting the cross-covariance matrix an ANM-based model has been proposed. We then prove that this model can be efficiently solved as a semi-definite programming (SDP). Secondly, a modified model has been presented to improve the estimation accuracy. It is shown that our proposed methods can be applied to both uniform and sparse L-shaped arrays and do not require any knowledge of the number of sources. Furthermore, since our methods greatly reduce the model size as compared to the conventional ANM method, and thus are much more efficient. Simulations results are provided to demonstrate the advantage of our methods.

Index Terms— 2-D DOA estimation, L-shaped array, atomic norm, cross-covariance matrix

1. INTRODUCTION

The problem of 2-dimensional (2-D) direction-of-arrival (DOA) estimation plays a fundamental role in array signal processing and is encountered in a variety of applications. These applications include, for instance, using an airborne or a spaceborne array to observe ground-based sources, or, estimating the channel of the massive multiple-input and multiple-output (MIMO) systems in wireless communications. In 2-D DOA estimation, the azimuth and elevation angles of the incident sources are jointly estimated by using planar arrays, which can be roughly classified into three categories: the rectangular arrays [1], the L/T-shaped arrays [2] and the cross arrays. The selection of the array geometry largely affects the estimation accuracy as well as the computational efficiency and has been extensively investigated in literature [2, 3]. In particular, the rectangular array can be regarded as the 2-D extension of the uniform linear array (ULA) and hence several computationally efficient methods have been proposed for 2-D DOA estimation in URAs [1, 4], among which the 2-D ESPRIT [4] is an easy-to-implement algorithm due to the shift invariance property of the array output. However, it is usually unapplicable to the L/T-shaped or cross arrays. The L-shaped array has the best estimation performance due to its larger array aperture as defined by the largest distance among the sensors [5]. Hence the L-shaped array has been often employed in dealing with 2-D DOA estimation problems and many methods have been proposed by exploring the structural information of the array geometry. In particular, the L-shaped array has an advantage that the cross-correlation matrix (CCM) between the received data of the two orthogonal ULAs can eliminate additive noises, based on which several methods have been proposed [2, 6, 7]. However, most of these methods have utilized the L-shaped array consisting of two ULAs, and hence they may suffer from the difficulty when some sensors are ”missing”. In addition, most of these methods rely on prior knowledge on the number of sources, which is actually unavailable in practice.

Recently, with the development of atomic norm theory, the atomic norm minimization (ANM) approach has been incorporated into the 2-D DOA estimation (a.k.a. the line spectral estimation) for super-resolution [8–10]. In particular, the ANM solves a semi-definite programming (SDP) problem by exploiting the structure of the two-level Toeplitz matrix. Compared to the conventional methods, the ANM method is immune to the correlation between the impinged source signals as well as the number of sources. Furthermore, it is shown that the angle ambiguity problem can be also solved [9], [11]. However, since ANM requires to solve an SDP problem, it incurs a high computational complexity, especially in the multi-snapshot case, which becomes near intractable for large-scale antennas systems. To deal with this problem, some latest studies decouple the two-level Toeplitz matrix into two Toeplitz matrices in one dimension [12, 13]. In this way, the new SDP formulation has a much reduced problem size and hence the computational efficiency can be improved. Nevertheless, this method can only handle single snapshot case and the extension to the multi-snapshot case is not straightforward.

This work was supported by the National Natural Science Foundation of China under grant No. 61372122, No. 61471205 and No. 61771256; the Innovation Program for Postgraduate in Jiangsu Province under grant No. KYLX 0813.

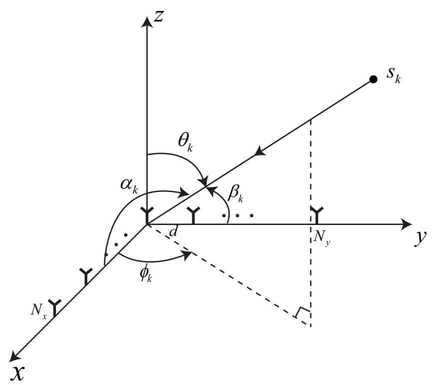

Fig. 1. Array geometry of the L-shaped array.

To the best of our knowledge, most of the existing ANM-based 2-D DOA estimation methods are proposed based on the uniform or sparse rectangular array. Although the ANM-based methods are applicable to the L-shaped array by regarding it as a special case of the sparse rectangular array, the characteristics of the L-shaped array are not fully exploited in these methods to improve the estimation performance. For instance, the coprime linear array can be a great alternative for each ULA in the L-shaped array [14–18]. In this paper, we propose an ANM-based model for L-shaped array by employing the CCM and prove that the model can be efficiently solved as an SDP. We then modify the constraint of the problem to improve its estimation performance. The proposed methods are computationally much more efficient than the conventional ANM method and can be applied to sparse L-shaped array, which is usually difficult for many other methods [2, 6, 7]. Simulations are carried out to validate the effectiveness of our methods.

2. SIGNAL MODEL

Suppose K far-field narrowband sources impinge onto an L-shaped array consisting of two ULAs with half-wavelength inter-element spacing as illustrated in Fig. 1. The ULAs along the x- and y-directions consist of N_x and N_y sensors, respectively. Note that the sensor at the origin is shared by the two ULAs, hence the total number of sensors in the L-shaped array is $N_x + N_y - 1$. In Fig. 1, the θ_k and ϕ_k denote the elevation and azimuth angles, respectively, and α_k and β_k denote the electrical angles in x- and y-directions of the k-th signal, respectively. From basic geometric knowledge, the electrical angles have the following relations with respect to elevation and azimuth angles,

$$\begin{aligned}\phi_k &= \tan^{-1}\left(\frac{\cos(\beta_k)}{\cos(\alpha_k)}\right)\\ \theta_k &= \sin^{-1}\left(\sqrt{\cos^2(\alpha_k)+\cos^2(\beta_k)}\right).\end{aligned} \tag{1}$$

Hence, when the electrical angles are retrieved, the elevation and azimuth angles can be uniquely determined by (1).

When L snapshots are collected, the array output can be formulated as,

$$\boldsymbol{X} = \boldsymbol{A}_x\boldsymbol{S} + \boldsymbol{V}_x, \tag{2}$$

$$\boldsymbol{Y} = \boldsymbol{A}_y\boldsymbol{S} + \boldsymbol{V}_y, \tag{3}$$

where $\boldsymbol{X}$ and $\boldsymbol{Y}$ are the array outputs along x- and y-directions, respectively, $\boldsymbol{A}_x = [\boldsymbol{a}_x(\alpha_1), \cdots, \boldsymbol{a}_x(\alpha_K)]$ and $\boldsymbol{A}_y = [\boldsymbol{a}_y(\beta_1), \cdots, \boldsymbol{a}_y(\beta_K)]$ are the manifold of the array along x- and y-directions, respectively, $\boldsymbol{S}$ denotes the waveform of the sources, and $\boldsymbol{V}_x$ and $\boldsymbol{V}_y$ are the additive noises received by the arrays along x- and y-directions, respectively.

The goal of 2-D DOA estimation is to estimate α_k and β_k given the array output $\boldsymbol{X}$ and $\boldsymbol{Y}$. In the following, we will exploit the structural information of the L-shaped array and provide a super-resolution approach based on the atomic norm theory.

3. THE PROPOSED METHOD

From (2) and (3), we can easily obtain the CCM of the array output as,

$$\boldsymbol{R} = E[\boldsymbol{Y}\boldsymbol{X}^H] = \boldsymbol{A}_y\boldsymbol{P}\boldsymbol{A}_x^H, \tag{4}$$

where $\boldsymbol{P} \triangleq E[\boldsymbol{S}\boldsymbol{S}^H] = \text{diag}(\boldsymbol{p})$ denotes the covariance matrix of the sources with $\boldsymbol{p} = [p_1, \cdots, p_K]^T$. Then, by vectorizing $\boldsymbol{R}$ column by column, we can have,

$$\boldsymbol{r} = \text{vec}(\boldsymbol{R}) = \sum_{k=1}^{K} p_k\boldsymbol{b}_k, \tag{5}$$

where $\boldsymbol{b}_k = \boldsymbol{a}_x^*(\alpha_k) \otimes \boldsymbol{a}_y(\beta_k)$. Inspired by the atomic norm theory, we formally construct the following atom set,

$$\mathcal{A} = \left\{\boldsymbol{b}_k = \boldsymbol{a}_x^*(\alpha_k) \otimes \boldsymbol{a}_y(\beta_k), \alpha_k, \beta_k \in [-90^\circ, 90^\circ)\right\}. \tag{6}$$

Then the 2-D DOA estimation can be accomplished by minimizing the following atomic norm,

$$\|\boldsymbol{r}\|_{\mathcal{A}} = \inf_{p_k,\alpha_k,\beta_k}\left\{\sum_k p_k : \boldsymbol{r} = \sum_k p_k\boldsymbol{b}_k, p_k \in \mathbb{R}^+, \boldsymbol{b}_k \in \mathcal{A}\right\}. \tag{7}$$

Although the atomic norm (7) is convex, it is a semi-infinite program with an infinite number of variables. To practically solve (7), inspired by Theorem 3 in [19], an SDP formulation of $\|\boldsymbol{r}\|_{\mathcal{A}}$ is provided in the following theorem.[1]

Theorem 1 *$\|\boldsymbol{r}\|_{\mathcal{A}}$ defined in (7) equals the optimal value of the following SDP:*

$$\begin{aligned}&\min_{\mathbb{T},t}\ \frac{1}{2\sqrt{N_xN_y}}(t + tr[\mathbb{T}])\\ &s.t.\ \begin{bmatrix} t & \boldsymbol{r}^H \\ \boldsymbol{r} & \mathbb{T}\end{bmatrix} \geq \boldsymbol{0},\end{aligned} \tag{8}$$

where $\mathbb{T}$ is a two-level Toeplitz matrix.

Proof: We first introduce the following lemma.

Lemma 1 ([20]) *Given $\boldsymbol{R} = \boldsymbol{B}\boldsymbol{B}^H \geq \boldsymbol{0}$, it holds that $\boldsymbol{r}^H\boldsymbol{R}^{-1}\boldsymbol{r} = \min\|\boldsymbol{p}\|_2^2$, subject to $\boldsymbol{B}\boldsymbol{p} = \boldsymbol{r}$.*

[1] Although a similar result is provided in [10], our proof is carried out from a different perspective and is simpler.

It follows from the constraint in (8) that $\mathbb{T} \geq \mathbf{0}$ and $t \geq \boldsymbol{r}^H \mathbb{T}^{-1} \boldsymbol{r}$. So, it suffices to show that

$$\|\boldsymbol{r}\|_{\mathcal{A}} = \min_{\mathbb{T}} \frac{1}{2\sqrt{N_x N_y}} (\text{tr}[\mathbb{T}] + \boldsymbol{r}^H \mathbb{T}^{-1} \boldsymbol{r}) \quad \text{s.t.}\ \mathbb{T} \geq \mathbf{0}. \tag{9}$$

Let $\mathbb{T} = \boldsymbol{B}\boldsymbol{C}\boldsymbol{B}^H = [\boldsymbol{B}\boldsymbol{C}^{\frac{1}{2}}][\boldsymbol{B}\boldsymbol{C}^{\frac{1}{2}}]^H$ be any feasible Vandermonde decomposition, where $\boldsymbol{B} = [\ldots, \boldsymbol{b}_k, \ldots]$ and $\boldsymbol{C} = \text{diag}(\ldots, c_k, \ldots)$ with $c_k > 0$. Hence we have $\text{tr}[\mathbb{T}] = N_x N_y \sum c_k$. According to Lemma 1, we have that

$$\begin{aligned} \boldsymbol{r}^H \mathbb{T}^{-1} \boldsymbol{r} &= \min_{\boldsymbol{v}} \|\boldsymbol{v}\|_2^2 \quad \text{s.t.}\ \boldsymbol{r} = \boldsymbol{B}\boldsymbol{C}^{\frac{1}{2}}\boldsymbol{v} \\ &= \min_{\boldsymbol{p}} \left\|\boldsymbol{C}^{-\frac{1}{2}}\boldsymbol{p}\right\|_2^2 \quad \text{s.t.}\ \boldsymbol{r} = \boldsymbol{B}\boldsymbol{p} \\ &= \min_{\boldsymbol{p}} \boldsymbol{p}^H \boldsymbol{C}^{-1} \boldsymbol{p} \quad \text{s.t.}\ \boldsymbol{r} = \boldsymbol{B}\boldsymbol{p}. \end{aligned} \tag{10}$$

Based on (10), we have,

$$\begin{aligned} &\min_{\mathbb{T}} \frac{1}{2\sqrt{N_x N_y}} (\text{tr}[\mathbb{T}] + \boldsymbol{r}^H \mathbb{T}^{-1} \boldsymbol{r}) \\ &= \min_{\substack{\boldsymbol{B}\boldsymbol{p}=\boldsymbol{r}, \\ \boldsymbol{p}, \boldsymbol{B}, c_n > 0}} \frac{\sqrt{N_x N_y}}{2} \sum_n c_n + \frac{1}{2\sqrt{N_x N_y}} \boldsymbol{p}^H \boldsymbol{C}^{-1} \boldsymbol{p} \\ &= \min_{\substack{\boldsymbol{B}\boldsymbol{p}=\boldsymbol{r}, \\ \boldsymbol{p}, \boldsymbol{B}, c_n > 0}} \frac{\sqrt{N_x N_y}}{2} \sum_n c_n + \frac{1}{2\sqrt{N_x N_y}} \sum_n p_n^2 c_n^{-1} \\ &= \min_{\boldsymbol{B}, \boldsymbol{p}} \sum_n p_n \quad \text{s.t.}\ \boldsymbol{B}\boldsymbol{p} = \boldsymbol{r} \\ &= \|\boldsymbol{r}\|_{\mathcal{A}}. \end{aligned} \tag{11}$$

Hence, Theorem 1 can be concluded. ■

Note that the CCM is usually obtained with limited snapshots as,

$$\widehat{\boldsymbol{R}} = \frac{1}{L} \boldsymbol{Y} \boldsymbol{X}^H, \tag{12}$$

where $\widehat{\boldsymbol{R}}$ is error-contaminated due to finite snapshots. We denote the error component as

$$\boldsymbol{E} = \widehat{\boldsymbol{R}} - \boldsymbol{R} \tag{13}$$

where $\boldsymbol{E}$ consists of signal-signal and signal-noise cross correlation terms which are non-zero due to finite snapshot effect. By taking this error component into consideration, we propose the following ANM approach,

$$\begin{aligned} &\min_{\mathbb{T}, t, \boldsymbol{r}} \frac{1}{2\sqrt{N_x N_y}} (t + \text{tr}[\mathbb{T}]) \\ &\text{s.t.} \begin{bmatrix} t & \boldsymbol{r}^H \\ \boldsymbol{r} & \mathbb{T} \end{bmatrix} \geq \mathbf{0}, \left\|\widehat{\boldsymbol{r}} - \boldsymbol{r}\right\|_2 \leq \eta, \end{aligned} \tag{14}$$

where $\widehat{\boldsymbol{r}} = \text{vec}(\widehat{\boldsymbol{R}})$ and $\eta \geq \|\boldsymbol{E}\|_F$ denotes the upper bound of the error energy.

Note that the DOAs of interest are actually encoded in the two-level Toeplitz matrix $\mathbb{T}$. As long as $\mathbb{T}$ is determined, the DOAs can be retrieved and automatically paired by using the generalized Vandermonde decomposition theorem given in [9].

Remark 1 *Compared to the ANM method in [9] and [10], which is time-consuming in the multiple snapshot case, our proposed method transforms the multiple snapshot model into the single snapshot model and the computational burden is greatly reduced as will be seen in simulations. Since we employ the CCM to eliminate the additive noise, the proposed method is named as cross-covariance ANM (CC-ANM).*

We now consider the sparse L-shaped array where some sensors of the two ULAs fail to function or are missing. Let us further define the sensor index sets of the two linear arrays as $\boldsymbol{\Omega}_x$ and $\boldsymbol{\Omega}_y$, respectively.[2] Let $\boldsymbol{\Gamma}_x$ be a selection matrix with respect to $\boldsymbol{\Omega}_x$ such that the m-th row of $\boldsymbol{\Gamma}_x$ contains all zeros but a single 1 at the Ω_{x_m}-th position where Ω_{x_m} is the m-th element in $\boldsymbol{\Omega}_x$. Similarly, we define $\boldsymbol{\Gamma}_y$. By definition, the sample CCM can be denoted as $\widehat{\boldsymbol{R}}_{\boldsymbol{\Omega}} = \boldsymbol{\Gamma}_y \widehat{\boldsymbol{R}} \boldsymbol{\Gamma}_x^H$ and its vectorized version is $\widehat{\boldsymbol{r}}_{\boldsymbol{\Omega}} = \text{vec}(\widehat{\boldsymbol{R}}_{\boldsymbol{\Omega}}) = (\boldsymbol{\Gamma}_x^T \otimes \boldsymbol{\Gamma}_y)\widehat{\boldsymbol{r}}$. Following the same manner as formulating problem (14), we propose the following SDP for the sparse L-shaped array,

$$\begin{aligned} &\min_{\mathbb{T}, t, \boldsymbol{r}} \frac{1}{2\sqrt{N_x N_y}} (t + \text{tr}[\mathbb{T}]) \\ &\text{s.t.} \begin{bmatrix} t & \boldsymbol{r}^H \\ \boldsymbol{r} & \mathbb{T} \end{bmatrix} \geq \mathbf{0}, \left\|\widehat{\boldsymbol{r}}_{\boldsymbol{\Omega}} - \boldsymbol{r}_{\boldsymbol{\Omega}}\right\|_2 \leq \eta, \end{aligned} \tag{15}$$

where $\boldsymbol{r}_{\boldsymbol{\Omega}} = (\boldsymbol{\Gamma}_x^T \otimes \boldsymbol{\Gamma}_y)\boldsymbol{r}$.

Remark 2 *From problem (15) it can be seen that, our proposed method is still applicable even if some of the sensors in ULAs fail and hence is more reliable for practical applications. Furthermore, based on the atomic norm theory, CC-ANM method does not require any knowledge of the number of sources.*

4. THE MODIFIED CC-ANM

Although problem (14) or (15) can be efficiently solved by using CVX in a polynomial time, the appropriate value of user-defined parameter η is usually hard to obtain. In this section, we propose a modified CC-ANM where the parameter can be easily determined. Note that $\boldsymbol{r}_{\boldsymbol{\Omega}} = \boldsymbol{r}$ when no sensor fails, hence model (14) can be regarded as a special case of model (15). Without loss of generality, we use model (15) in this section and give the following theorem.

Theorem 2 *Suppose that the error component is given as $\boldsymbol{\varepsilon}_{\boldsymbol{\Omega}} = \widehat{\boldsymbol{r}}_{\boldsymbol{\Omega}} - \boldsymbol{r}_{\boldsymbol{\Omega}}$, $\boldsymbol{R}_{\boldsymbol{\Omega}_x}$ and $\boldsymbol{R}_{\boldsymbol{\Omega}_y}$ are the covariance matrix of the linear arrays along x- and y-directions, respectively. Then, $\boldsymbol{\varepsilon}_{\boldsymbol{\Omega}}$ obeys the following asymptotic Gaussian distribution,*

$$\boldsymbol{\varepsilon}_{\boldsymbol{\Omega}} \sim AsN(\mathbf{0}, \boldsymbol{Q}), \tag{16}$$

where $\boldsymbol{Q} = \frac{1}{L} \boldsymbol{R}_{\boldsymbol{\Omega}_x}^T \otimes \boldsymbol{R}_{\boldsymbol{\Omega}_y}$.

Proof: Inspired by [23], we first denote the i-th subvector (with length of M_y) of $\widehat{\boldsymbol{r}}_{\boldsymbol{\Omega}}$ as [3]

$$[\widehat{\boldsymbol{r}}_{\boldsymbol{\Omega}}]_i = \frac{1}{L} \sum_{t=1}^{L} \boldsymbol{y}(t) \boldsymbol{x}_i^*(t). \tag{17}$$

[2] Detailed description of the sensor index set can be found in [21,22].

[3] M_x, M_y denote the number of sensors along x- and y-directions, respectively.

Then we can establish the following relation,

$$
\begin{aligned}
E\left[[\widehat{\boldsymbol{r}}_{\boldsymbol{\Omega}}]_i[\widehat{\boldsymbol{r}}_{\boldsymbol{\Omega}}]_j^H\right] &= \frac{1}{L^2}\sum_{t=1}^{L}\sum_{s=1}^{L} E[\boldsymbol{y}(t)\boldsymbol{x}_i^*(t)\boldsymbol{y}(s)^*\boldsymbol{x}_j(s)] \\
&= [\boldsymbol{r}_{\boldsymbol{\Omega}}]_i[\boldsymbol{r}_{\boldsymbol{\Omega}}]_j^H + \frac{1}{L}[\boldsymbol{R}_{\boldsymbol{\Omega}_x}]_{ji}\boldsymbol{R}_{\boldsymbol{\Omega}_y},
\end{aligned}
\tag{18}
$$

from which it can be concluded that,

$$
\begin{aligned}
\boldsymbol{Q} &= E[(\widehat{\boldsymbol{r}}_{\boldsymbol{\Omega}} - \boldsymbol{r}_{\boldsymbol{\Omega}})(\widehat{\boldsymbol{r}}_{\boldsymbol{\Omega}} - \boldsymbol{r}_{\boldsymbol{\Omega}})^H] \\
&= \frac{1}{L}\boldsymbol{R}_{\boldsymbol{\Omega}_x}^T \otimes \boldsymbol{R}_{\boldsymbol{\Omega}_y}.
\end{aligned}
\tag{19}
$$

■

According to Theorem 2, we can show that $\boldsymbol{Q}^{-\frac{1}{2}}\boldsymbol{\varepsilon}_{\boldsymbol{\Omega}}$ satisfies the standard Gaussian distribution, i.e., $AsN(\boldsymbol{0}, \boldsymbol{I})$, and its ℓ_2-norm satisfies the chi-square distribution as,

$$
\left\|\boldsymbol{Q}^{-\frac{1}{2}}\boldsymbol{\varepsilon}_{\boldsymbol{\Omega}}\right\|_2^2 \sim As\chi^2(M_xM_y). \tag{20}
$$

Based on the property of the chi-square distribution, the following inequality holds with probability $1-\kappa$,

$$
\left\|\boldsymbol{Q}^{-\frac{1}{2}}\boldsymbol{\varepsilon}_{\boldsymbol{\Omega}}\right\|_2 \leq \beta, \tag{21}
$$

where κ is usually chosen to be a small value (e.g., 10^{-4}) and β can be determined by using the Matlab routine chi2inv$(1-\kappa, M_xM_y)$. Equation (21) can be regarded as the weighted least squares criterion and is a large-snapshot approximation to the maximum likelihood criterion [23]. As a result, we have the following modified SDP,

$$
\begin{aligned}
&\min_{\mathbb{T},t,\boldsymbol{r}} \frac{1}{2\sqrt{N_xN_y}}(t + \text{tr}[\mathbb{T}]) \\
&\text{s.t.} \begin{bmatrix} t & \boldsymbol{r}^H \\ \boldsymbol{r} & \mathbb{T} \end{bmatrix} \geq \boldsymbol{0}, \left\|\boldsymbol{Q}^{-\frac{1}{2}}\boldsymbol{\varepsilon}_{\boldsymbol{\Omega}}\right\|_2 \leq \beta.
\end{aligned}
\tag{22}
$$

After obtaining $\mathbb{T}$, the DOAs can be retrieved accordingly. We name the proposed method as modified CC-ANM (MCC-ANM).

Before closing this section, we give a complexity comparison between our method and the traditional ANM method. In particular, the computational complexity of the traditional ANM method is $O(n_1^2n_2^{2.5})$, where $n_1 = L^2 + P$ and $n_2 = L + M_xM_y$ with $P = 2M_xM_y - M_x - M_y + 1$ being the number of variables in $\mathbb{T}$. While in our methods, the computational complexity can be greatly reduced by noting that $n_1 = 1 + P$ and $n_2 = 1 + M_xM_y$. The superiority of our method will be further shown in the next section.

5. NUMERICAL RESULTS

In this section, two L-shaped arrays are considered for simulations: one consisting of two 5-element ULAs (*Array 1*) and the other consisting of two sparse linear arrays with $\boldsymbol{\Omega}_x = \boldsymbol{\Omega}_y = \{1, 2, 3, 5\}$ (*Array 2*). We compare our proposed methods with ANM [9], which is the state-of-the-art gridless method for 2-D DOA estimation. All the compared methods are implemented by SDPT3.

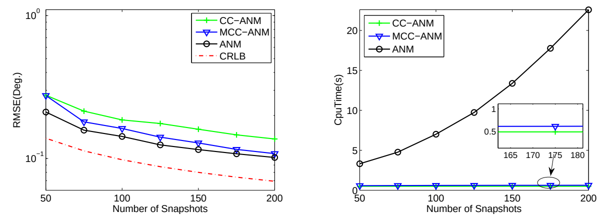

(a) RMSE (b) CPU time

Fig. 2. RMSE and CPU time comparisons with *Array 1*.

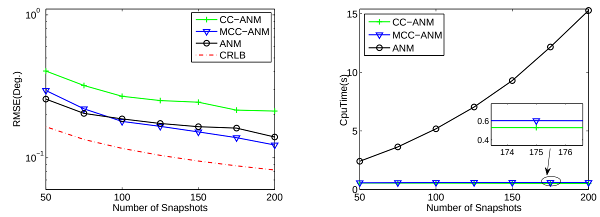

(a) RMSE (b) CPU time

Fig. 3. RMSE and CPU time comparisons with *Array 2*.

Suppose two source signals impinge onto *Array 1* from $\boldsymbol{\alpha} = [-25°, 30°]$ and $\boldsymbol{\beta} = [-35°, 0°]$. We examine the performance of our methods with comparison to ANM in terms of RMSE and CPU time, respectively. The SNR is set to 10dB and the number of snapshots varies from 50 to 200. We carry out 400 independent trials and show the statistical results in Fig. 2. From Fig. 2 (a), it can be seen that, the performance of these three methods is in general improved as the number of snapshots grows. Due to the modified constraint, MCC-ANM is superior to CC-ANM. Also, the performance gap between ANM and MCC-ANM becomes smaller when L gets large. Although ANM shows the best estimation performance, its computational workload can be unaffordable (especially when L is large) as shown in Fig. 2 (b). On the other hand, the computational complexity of our proposed methods is immune to the number of snapshots.

We then use *Array 2* to replace *Array 1* and carry out the previous experiment with the same settings. The simulation results are provided in Fig. 3. Clearly, MCC-ANM gives a better estimation performance than ANM does when L is large enough. More importantly, our proposed methods are much more computationally efficient than ANM in terms of the running time comparison.

6. CONCLUSION

In this paper, we have addressed the 2-D DOA estimation problem in the scenario of L-shaped arrays. By exploiting the characteristics of the L-shaped array, two gridless methods which can be applied to both uniform and sparse L-shaped arrays have been proposed. Simulation results show that our methods provide similar estimation performance to ANM method but with a much smaller computational workload.

7. REFERENCES

[1] P. Heidenreich, A. M. Zoubir, and M. Rubsamen, "Joint 2-D DOA estimation and phase calibration for uniform rectangular arrays," *IEEE Transactions on Signal Processing*, vol. 60, no. 9, pp. 4683–4693, Sept 2012.

[2] J. F. Gu and P. Wei, "Joint SVD of two cross-correlation matrices to achieve automatic pairing in 2-D angle estimation problems," *IEEE Antennas and Wireless Propagation Letters*, vol. 6, pp. 553–556, 2007.

[3] M. G. Porozantzidou and M. T. Chryssomallis, "Azimuth and elevation angles estimation using 2-D music algorithm with an L-shape antenna," in *2010 IEEE Antennas and Propagation Society International Symposium*, July 2010, pp. 1–4.

[4] M. D. Zoltowski, M. Haardt, and C. P. Mathews, "Closed-form 2-D angle estimation with rectangular arrays in element space or beamspace via unitary esprit," *IEEE Transactions on Signal Processing*, vol. 44, no. 2, pp. 316–328, Feb 1996.

[5] Y. Hua, T. K. Sarkar, and D. D. Weiner, "An L-shaped array for estimating 2-D directions of wave arrival," *IEEE Transactions on Antennas and Propagation*, vol. 39, no. 2, pp. 143–146, Feb 1991.

[6] G. Wang, J. Xin, N. Zheng, and A. Sano, "Computationally efficient subspace-based method for two-dimensional direction estimation with L-shaped array," *IEEE Transactions on Signal Processing*, vol. 59, no. 7, pp. 3197–3212, July 2011.

[7] N. Tayem and H. M. Kwon, "L-shape 2-dimensional arrival angle estimation with propagator method," in *2005 IEEE 61st Vehicular Technology Conference*, May 2005, vol. 1, pp. 6–10 Vol. 1.

[8] W. Xu, J. F. Cai, K. V. Mishra, M. Cho, and A. Kruger, "Precise semidefinite programming formulation of atomic norm minimization for recovering d-dimensional ($d \geq 2$) off-the-grid frequencies," in *2014 Information Theory and Applications Workshop (ITA)*, Feb 2014, pp. 1–4.

[9] Z. Yang, L. Xie, and P. Stoica, "Vandermonde decomposition of multilevel toeplitz matrices with application to multidimensional super-resolution," *IEEE Transactions on Information Theory*, vol. 62, no. 6, pp. 3685–3701, June 2016.

[10] Y. Chi and Y. Chen, "Compressive two-dimensional harmonic retrieval via atomic norm minimization," *IEEE Transactions on Signal Processing*, vol. 63, no. 4, pp. 1030–1042, Feb 2015.

[11] X. Wu, W. P. Zhu, and J. Yan, "A fast covariance matrix reconstruction method for two-dimensional direction-of-arrival estimation," in *2017 IEEE International Conference on Acoustics, Speech and Signal Processing (I-CASSP)*, March 2017, pp. 3166–3170.

[12] Z. Tian, Z. Zhang, and Y. Wang, "Low-complexity optimization for two-dimensional direction-of-arrival estimation via decoupled atomic norm minimization," in *2017 IEEE International Conference on Acoustics, Speech and Signal Processing (ICASSP)*, March 2017, pp. 3071–3075.

[13] J. F. Cai, W. Xu, and Y. Yang, "Large scale 2D spectral compressed sensing in continuous domain," in *2017 IEEE International Conference on Acoustics, Speech and Signal Processing (ICASSP)*, March 2017, pp. 5905–5909.

[14] P. Pal and P. P. Vaidyanathan, "Coprime sampling and the music algorithm," in *Digital Signal Processing Workshop and IEEE Signal Processing Education Workshop (DSP/SPE), 2011 IEEE*, Jan 2011, pp. 289–294.

[15] C. Zhou, Y. Gu, S. He, and Z. Shi, "A robust and efficient algorithm for coprime array adaptive beamforming," *IEEE Transactions on Vehicular Technology*, vol. PP, no. 99, pp. 1–1, 2017.

[16] Z. Shi, C. Zhou, Y. Gu, N. A. Goodman, and F. Qu, "Source estimation using coprime array: A sparse reconstruction perspective," *IEEE Sensors Journal*, vol. 17, no. 3, pp. 755–765, Feb 2017.

[17] C. Zhou, Y. Gu, Y. D. Zhang, Z. Shi, T. Jin, and X. Wu, "Compressive sensing based coprime array direction-of-arrival estimation," *IET Communications*, vol. 11, no. 11, pp. 1719–1724, Aug 2017.

[18] C. Zhou and J. Zhou, "Direction-of-arrival estimation with coarray esprit for coprime array," *Sensors*, vol. 17, no. 8, 2017.

[19] Z. Yang and L. Xie, "Exact joint sparse frequency recovery via optimization methods," *IEEE Transactions on Signal Processing*, vol. 64, no. 19, pp. 5145–5157, Oct 2016.

[20] Z. Yang and L. Xie, "On gridless sparse methods for line spectral estimation from complete and incomplete data," *IEEE Transactions on Signal Processing*, vol. 63, no. 12, pp. 3139–3153, June 2015.

[21] X. Wu, W. P. Zhu, and J. Yan, "A Toeplitz covariance matrix reconstruction approach for direction-of-arrival estimation," *IEEE Transactions on Vehicular Technology*, vol. 66, no. 9, pp. 8223–8237, Sept 2017.

[22] X. Wu, W. P. Zhu, and J. Yan, "Direction-of-arrival estimation based on Toeplitz covariance matrix reconstruction," in *2016 IEEE International Conference on Acoustics, Speech and Signal Processing (ICASSP)*, March 2016, pp. 3071–3075.

[23] Björn Ottersten, Peter Stoica, and Richard Roy, "Covariance matching estimation techniques for array signal processing applications," *Digital Signal Processing*, vol. 8, no. 3, pp. 185–210, 1998.